

Organic Pigment Nanoparticle Thin Film Devices via Lewis Acid Pigment Solubilization

Bing R. Hsieh* and Andrew R. Melnyk

Xerox Corporation, 800 Phillips Road, 114-39D,
Webster, New York 14580

Received December 30, 1997

Revised Manuscript Received June 25, 1998

Organic dyes and pigments have a wide range of commercial applications in coatings, printing, information storage, and display technologies.¹ Pigments have many advantages over dyes, such as light and water fastness, color strength, photosensitivity, and overall stability. However, pigments are more difficult to handle and process than dyes, mainly because pigments are highly insoluble. The available processes for the deposition of pigment thin films needed for the variety of applications have been complicated and limited. Three most commonly used processes are high-energy pigment attrition, sulfuric acid pasting and flushing of pigment, and the pigment sublimation. The pigment dispersions obtained from the first two processes are then used to cast pigmented layers. Although fine pigment particles can be obtained, the resulting pigment dispersions often reaggregate in time. Pigment sublimation can give pigment layers with high purity and uniformity; however, it is a complicated and expensive manufacturing proposition, particularly for large-scale production operations. In addition to the above physical processes, chemical processes such as side chain routes and precursor routes have also been used to overcoming the processibility problems of pigments. The former involves the direct attachment of flexible or bulky substituents onto pigment molecules via stepwise organic synthesis.² The later involves the preparation of a soluble precursor which can be converted to the insoluble parent pigment by heat or radiation, such as the latent pigment work reported recently for pyrrolo-[3,4-C]pyrroles.³ We have used these two chemical processes to overcome the processibility issue associated with conjugated polymers such as poly(*p*-phenylenevinylenes).⁴ However, the chemical processes are often system specific and are thus less general than the physical processes.

Here we report a new physical process, namely Lewis acid pigment solubilization (LAPS), for the deposition

of pigment thin films composed of pigment nanoparticles. The process involves the solubilization of a pigment in a Lewis acid/nitromethane solution. The resulting solution is used to cast pigment/Lewis acid thin films on substrates with a predeposited adhesive layer. The pigment thin films are then washed with aqueous solutions to remove the Lewis acid and give the final pigmented layers. This process is an adaptation of Lewis acid polymer solubilization for depositing rigid rod heterocyclic polymer thin films.⁵ We have found that LAPS is generally applicable to many heterocyclic pigment classes such as phthalocyanines, perylenebismidazoles, azos, and the like.⁶ As a result, these pigments can be processed like dyes at molecular level, defying the common definitions of dyes and pigments. We demonstrate in this paper the use of LAPS to fabricate multilayered organic photoconductors (OPC) with good sensitivity, high cyclic stability, low dark decay, and residual charges. We envision that LAPS has a tremendous potential for the fabrication of other pigment-based organic semiconductor devices such as light-emitting diodes,^{7–8} photodiodes, solar cells,⁹ and field effect transistors.¹⁰

Although a wide range of heterocyclic pigments have been dissolved by LAPS, we use one of the most photosensitive and stable pigments, namely bisbenzimidazole perylene^{11,12} (BZP, structure shown in Figure 1) to illustrate the typical LAPS procedure and for our study. A solution or a mixture of BZP and aluminum chloride (AlCl₃) was prepared by magnetically stirring a mixture of BZP, AlCl₃, nitromethane, and methylene chloride in 20 mL vials in a glovebox under nitrogen atmosphere for 12 h to give a pigment/AlCl₃ solution or a pigment/AlCl₃ mixture, depending on the pigment concentration. Table 1 summarizes the compositions for three representative BZP solution mixtures. The molar ratio of BZP to AlCl₃ was 1:6 in all cases. Solution 1, having about 2 wt % BZP, was easily filtered through a 0.45 μm filter; but solutions 2 and 3 with higher pigment concentrations could not be easily filtered. There was no scattering of light from solution 1; while there was scattering of light from solutions 2 and 3. This indicates that BZP can be completely solubilized at about 2 wt % and that BZP/AlCl₃ complex may form aggregates at

(1) Zollinger, H. *Color Chemistry*; VCH: New York, 1987. (b) P. Gregory, "High-Technology Applications of Organic Colorants", Plenum Press: NY, 1991; (c) P. Gregory, "Chemistry and Technology of Printing and Imaging Systems", Blackie Academic and Professional, London, 1996.

(2) Müllen, K.; Quante, H.; Benfaremo, N. In *Polymeric Materials Encyclopedia*; Salamone, J. C., Ed.; CRC Press: Boca Raton, FL, 1996; p 4999. (b) Leznoff, C. C.; Lever, A. B. P., Eds. *Phthalocyanines*; VCH publishers, Inc: New York, 1989. (c) Thomas, A. L. *Phthalocyanine Research and Applications*; CRC Press: Boca Raton, FL, 1990.

(3) Zmbounis, J. S.; Hao, Z.; Iqbal, A. *Nature* **1997**, *388*, 131. (b) Zmbounis, J. S.; Hao, Z.; Iqbal, A. U.S. Patent 5,616,725, 1997, and references therein.

(4) Hsieh, B. R.; Yu, Y.; VanLaeken, A. Lee, H. *Macromolecules* **1997**, *30*, 8094. (b) Hsieh, B. R.; Yu, Y.; Forsythe, E. W.; Schaaf, G. M.; Feld, W. A. *J. Am. Chem. Soc.* **1998**, *120*, 231.

(5) Jenekhe, S. A. U.S. patent 4,963,616, 1990. (b) Jenekhe, S. A. U.S. patent 4,945,156, 1990. (c) Jenekhe, S. A.; Johnson, P. O. *Macromolecules* **1990**, *23*, 4419.

(6) Hsieh, B. R.; Morrison, I. D.; Grabowski, E. F.; Melnyk, A. R. U.S. patent 5,405,724, 1995.

(7) Wakimoto, T.; Murayama, R.; Nakada, H.; Nomura, M.; Sato, G. U.S. Patent 5,276,381, 1994.

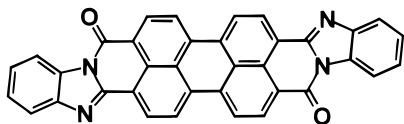
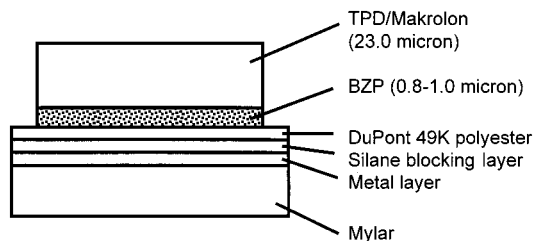
(8) Tang, C. W.; Van Slyke, S. A. *Appl. Phys. Lett.* **1987**, *51*, 913.

(b) Tang, W.; Van Slyke, S. A.; Chen, C. H. *J. Appl. Phys.* **1989**, *65*, 3610.

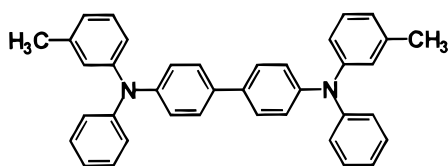
(9) Tang, C. W. *Appl. Phys. Lett.* **1986**, *48*, 183. (b) Antoniadis, H.; Hsieh, B. R.; Abkowitz, M. A.; Jenekhe, S. A.; Stolka, M. *Synth. Met.* **1994**, *62*, 265. (c) O'Regan, ; Grätzel, M. *Nature* **1991**, *353*, 737.

(10) Garnier, F.; Horowitz, G.; Peng, X.; Fichou, D. *Adv. Mater.* **1990**, *2*, 592. (b) Horowitz, G. *Adv. Mater.* **1990**, *2*, 287. (c) Garnier, F.; Hajlaoui, R.; Yassar, A.; Srivastava, P. *Science* **1994**, *265*, 1684. (d) Dodabalapur, A.; Torsi, L.; Katz, H. E. *Science* **1995**, *268*, 270. (e) Dodabalapur, A.; Katz, H. E.; Torsi, L.; Haddon, R. C. *Science* **1995**, *269*, 1560.

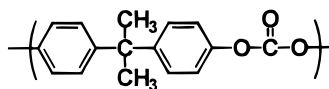
(11) Law, K. Y. *Chem. Rev.* **1993**, *93*, 449, and references therein. (12) Loutfy, R. O.; Hor, A. M.; Kazmaier, P.; Tam, M. *J. Imaging Sci.* **1989**, *33*, 151.



trans-BZP
(cis form not shown)



TPD



Makrolon

Figure 1. A typical OPC device structure and the chemical structures of BZP and TPD.

Table 1. Compositions of BZP/AlCl₃ Solutions

pigment & reagents	solution 1	solution 2	solution 3
BZP (g)	0.26	0.39	0.52
AlCl ₃ (g)	0.39	0.59	0.78
nitromethane (mL)	6	6	6
MeCl ₂ (mL)	4	4	4
BZP (wt %)	2.0	3.0	3.9

higher pigment concentrations. Being in complete solution, solution 1 should enable one to deposit thin films with the highest degree of uniformity and controlled thicknesses by means of spray or dip coating. However, we were limited to draw bar coating and thus chose the unfiltered solution #3 for the fabrication of OPC devices in order to achieve BZP layers (0.8–1.0 μm) with suitable optical density.

Metallized Mylar (75 μm) substrates were overcoated with a thin (20–50 nm) 2-aminopropyltriethoxysilane priming layer and then an adhesive layer of the DuPont 49 K polyester. A Gardner mechanically driven film applicator enclosed in a plexiglass acrylic box with an attached cover was used for depositing BZP/AlCl₃ layers onto the substrates using the BZP/AlCl₃ solution or mixture. The as-cast BZP/AlCl₃ layers were washed in a water tray for 5 min, followed by a second wash for 5 min either with 2% sodium carbonate (Na₂CO₃), with 2% ammonium hydroxide (NH₄OH), or with deionized water at 50 °C and then air-dried to give BZP charge generation layers. The transport layers (23.0 μm) were

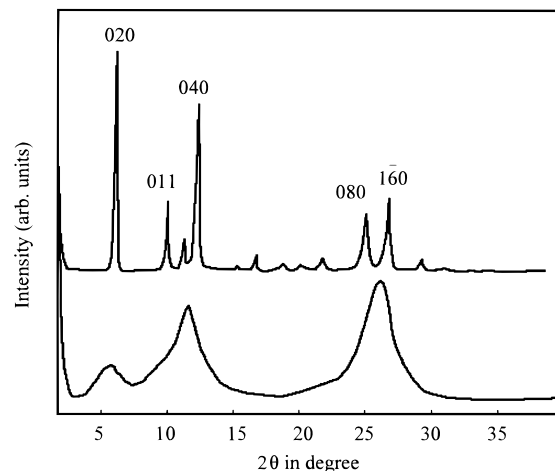


Figure 2. The X-ray diffraction patterns for attrited BZP (top) and LAPS-deposited BZP (bottom).

then deposited by draw bar coating using a solution of *N,N*-diphenyl-*N,N*-bis(*m*-tolyl)-1,1'-biphenyl-4,4'-diamine (TPD, shown in Figure 1, 5.0 g), Makrolon (5.0 g), and methylene chloride (57 g) to give OPC devices with the structure depicted in Figure 1.

Scanning electron micrographs of the pigment layers showed highly coherent filmlike images with no detectable individual pigment particles, indicating a very high degree of uniformity for the pigment layers. As shown in Figure 2, BZP layers deposited via LAPS showed significantly broader X-ray diffraction peaks than those for attrited and sublimed BZP.¹² From the X-ray diffraction patterns, we estimated an average crystallite size of about 50 nm, which is at least five times smaller than that for the attrited or sublimed BZP.¹³ One may expect even smaller crystallite sizes for spray-coated BZP layers based on solution 1. Our approach may represent the first example of depositing thin films of organic pigment nanoparticles.

Xerographic measurements¹⁴ were performed on three similar BZP OPC devices, I–III. The BZP layers in these devices were, respectively, subsequently washed with 2% Na₂CO₃, with 2% NH₄OH, or with deionized water at 50 °C. Figure 3 is an example of the voltage

(13) The crystallite size was derived from the Scherrer equation: $\tau = K\lambda/\beta \cos \theta$ where $K = 0.9$ is the shape factor, τ is the mean crystallite size, $\lambda = 1.5418$ is the wavelength of Cu K α radiation, β is the full-width at half-maximum for a given peak in radians, and θ is the peak position in degrees. The crystallite size for the sublimed BZP of about 170 nm was obtained by averaging the τ values for the five labeled peaks shown in Figure 2 and the crystallite size of about 50 nm for the LAPS deposited BZP was obtained by averaging the τ values for the three broad peaks shown in Figure 2. More detailed information can be obtained: Jenkins, R.; Snyder, R. L. *Introduction to X-ray Powder Diffractometry*; Wiley and Sons: New York, 1996.

(14) Xerographic measurements were made on a (rotating) cycling scanner at 20 rpm, 20 °C, and 35% RH, using 3 × 4 in samples of the imaging member prepared as described herein. The samples were corona-charged with a negative, constant current to an average charge of 105 nC/cm², which is equivalent to an electric field of 40 V/μm. The surface potential of the samples was monitored with Monroe Electronics noncontacting voltmeters (Model 144) placed at various positions around the circumference of the drum, corresponding to various times from charging. An exposure to monochromatic light was located 45° from charging or 0.375 s after charging and a white light erasure located 2.53 s after charging. Voltage probes were located to monitor the voltages after exposure and erase. The test sequence and data collection were controlled by computer. Monochromatic light exposure consisted of a collimated xenon lamp, first-order interference filters with a 10 nm halfwidth, neutral density filters to control the intensity of the light, a shutter, and a beam splitter with a calibrated PIN Si diode monitoring the exposure.

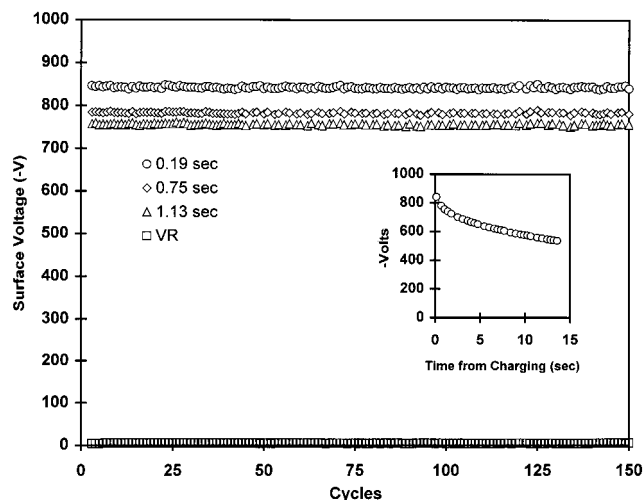


Figure 3. Example of cycling voltage data for device I and the corresponding dark discharge (inset).

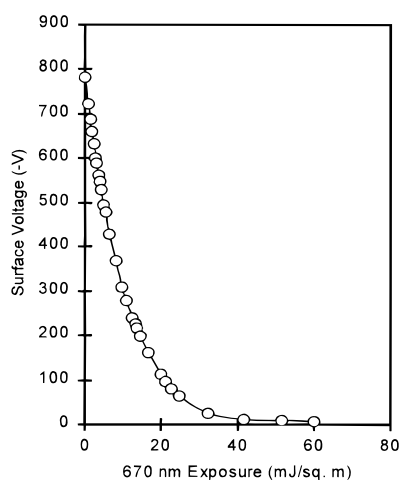


Figure 4. Photodischarge for 670 nm light, measured 0.375 s after exposure for device I.

with cycling for device I, showing four voltages, three measured after charging and one after light erasure. As is evident in Figure 3, the voltages are exceptionally stable with cycling; the random variation of less than 10 V is due to 1% variation in the corotron charging, and systematic variation in voltage is less than 1 V. Over 1000 cumulative cycles, the voltage changed by less than 10 V under constant charge conditions. The residual voltage remained at less than 5 V over the entire 1000 cycle test. The dark discharge was monitored by turning off the erase light and charging and observing the voltage over several cycles. The inset of Figure 3 shows the dark discharge, with an average dark discharge over 10 s of 27 V/s.

Figure 4 is a discharge curve observed 0.75 s after charging and 0.375 s after exposure to 670 nm light for device I. The slope of discharge (S), which corresponds to the sensitivity of the device, is 60 V/erg/cm², and the light exposures required to discharge from 800 to 400 V ($E_{0.5}$) or to 100 V ($E_{0.12}$) are 9 or 21 erg/cm², respectively, as shown in Table 2. The exposure is inversely proportional to the photosensitivity. The residual voltage, V_R ; the initial voltage (voltage 0.2 s after charging), $V_{0.2}$; and the 1 s dark discharge are also given in Table 2. Similar xerographic testing was

Table 2. Xerographic Data^a

device no.	V_R	$V_{0.2}$	dark decay (V/s)	sensitivity at 670 nm		
				S	$E_{0.5}$	$E_{0.12}$
I	4	845	27	60	9	21
II	5	885	15	32	15	35
III	5	864	23	50	11	24

^a V_R = residual voltage (in V). $V_{0.2}$ = the initial surface potential measured at 0.2 s (in V). S = the initial slope of the discharge curve (in V/erg/cm²). $E_{0.5}$ = the light exposure required to discharge from 800 to 400 V (in erg/cm²). $E_{0.12}$ = the light exposure required to discharge from 800 to 100 V (in erg/cm²).

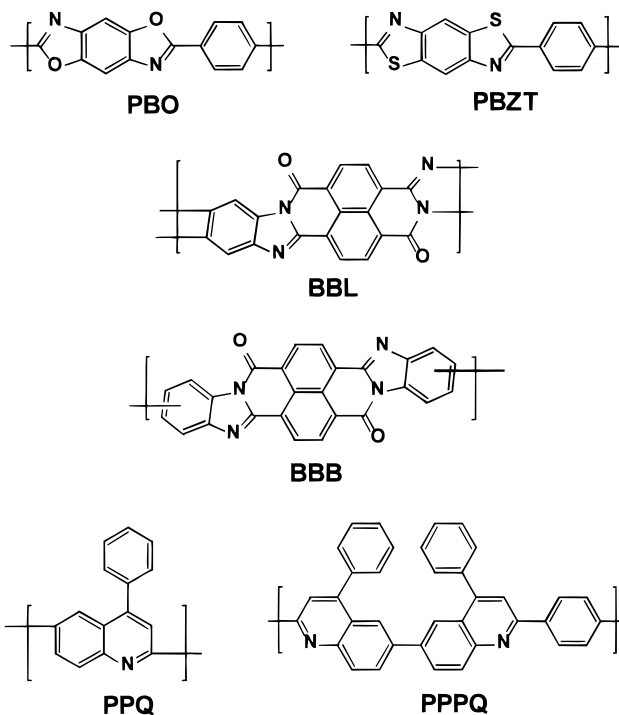


Figure 5. Structures and the corresponding acronyms for selected heterocyclic polymers that can be used as binders for the organic pigment nanoparticles.

performed for devices II and III and the resulting data are listed accordingly.

The different xerographic data for the three devices are likely to be related to the different aqueous washing methods. The Na₂CO₃-washed device I showed the highest sensitivity, while the NH₄OH-washed device II showed the lowest sensitivity. Devices based on BZP layers that were washed once with water showed xerographic data similar to that of device III, indicating that the second water wash has little effect on the device properties. Extremely rapid dark decay was found for a device based on a BZP/AlCl₃ layer which was not water washed, indicating that the impurities due to AlCl₃ can contribute to dark decay. Although the sensitivity of device I is still lower than that for the sublimed PZC OPC with $E_{0.5}$ of 3.5 erg/cm² reported by Loutfy et al.,¹² one should be able to optimize the sensitivity of the LAPS OPC through fine-tuning the coating and the washing parameters.

Dispersing organic pigment nanoparticles in an electrophotocurable polymer binder is an interesting combination. Heterocyclic ladder polymers such as those shown in Figure 5 are ideal binders for this purpose because they can be dissolved in Lewis acids/nitromethane as well.⁵ Devices with BZP/BBL as the

charge generation layer have been fabricated via LAPS and showed xerographic properties similar to those of BZP based devices.

In conclusion, LAPS is a new physical method for pigment processing in addition to pigment attrition, acid pasting, and pigment sublimation and may be the first approach for the deposition of organic pigment nano-

particles thin films. The fact that pigment can be dissolved in organic solvents is blurring the common definition of dyes and pigments. We envision tremendous potentials for LAPS in wide range of organic semiconductor device applications.

CM970823W